

# Localise to segment: crop to improve organ at risk segmentation accuracy

Abraham George Smith<sup>1, 2, \*</sup>, Denis Kutnár<sup>1, 2</sup>, Ivan Richter Vogelius<sup>2</sup>, Sune Darkner<sup>1</sup>, and Jens Petersen<sup>1, 2</sup>

<sup>1</sup>*Department of Computer Science, University of Copenhagen*

<sup>2</sup>*Department of Oncology, Rigshospitalet, University of Copenhagen*

\**ags@di.ku.dk*

## Abstract

Increased organ at risk segmentation accuracy is required to reduce cost and complications for patients receiving radiotherapy treatment. Some deep learning methods for the segmentation of organs at risk use a two stage process where a localisation network first crops an image to the relevant region and then a locally specialised network segments the cropped organ of interest. We investigate the accuracy improvements brought about by such a localisation stage by comparing to a single-stage baseline network trained on full resolution images. We find that localisation approaches can improve both training time and stability and a two stage process involving both a localisation and organ segmentation network provides a significant increase in segmentation accuracy for the spleen, pancreas and heart from the Medical Segmentation Decathlon dataset. We also observe increased benefits of localisation for smaller organs. Source code that recreates the main results is available at this [https](https://github.com/abrahamgeorge/Localise-to-segment) URL.

## Introduction

More than 50% of cancer patients receive radiotherapy which is associated with a range of dose dependent side effects. Delineation of organs at risk on treatment planning scans is crucial to minimise complications [8, 19]. Manual delineation is possible and still widely used but in comparison to automated methods is time consuming [32] and subject to large inter-observer variation [15]. Therefore, methods to improve the accuracy of automated methods are required. A review of auto-segmentation methods for radiotherapy is presented by Cardenas et al. [5] with deep learning methods and convolutional neural networks in particular representing the state-of-the-art.

Organ localisation has been used for a variety of tasks in image analysis and can reportedly improve segmentation accuracy whilst reducing computational memory and processing time requirements [37].

Kutnar et al. [17] found a two-stage localisation approach to be effective for the segmentation of lacunes in brain MR images and Gros et al. [10] found spine centerline localisation to provide state-of-the-art spinal cord segmentation accuracy. Feng et al. [9] proposed a two stage approach using cropped 3D images, where a similar 3D U-Net was used for both the initial organ localisation and segmentation stages. They claim their approach is more data efficient due to the use of voxel labels in the training of the localisation network. The method proposed by Feng et al. [9] is appealing as it uses the same method (segmentation with 3D-U-Net [6]) for both localisation and segmentation which simplifies both concept and implementation.

Although the method obtains competitive accuracy [39], an ablation analysis or baseline comparison method is lacking. Therefore, we conduct a more focused investigation to measure the accuracy gains brought about by such an approach to localisation. We hypothesise that localisation will improve organ at risk segmentation accuracy, demonstrated by a significant increase in dice. To the best of our knowledge, this hypothesis has not been tested in a focused investigation.

## Method

### Dataset

To evaluate the effect of localisation on a diverse array of organ at risk segmentation tasks, we used the spleen, pancreas, prostate, liver and heart (left atrium) datasets [25] from the Medical Segmentation Decathlon [2]. We used only the original training sets, as this portion of the data has corresponding labels available for download. To facilitate the training and evaluation of deep learning models for image segmentation, we split the downloaded images and labels into our own training, validation and test subsets with sizes of 60%, 20% and 20%, respectively (Table 1). This ratio between training, validation and test data was chosen as it is typical for deep learning model training.

Table 1: Number of images included in each of the training, validation and test datasets for each of the organs.

organ	training	validation	test
spleen	25	8	8
pancreas	169	56	56
prostate	19	7	6
liver	41	14	14
heart	12	4	4

## Implementation

We used PyTorch [22] (Version 1.13.1) and implemented a 3D U-Net [6] which is an encoder-decoder style semantic-segmentation architecture. For all experiments we use 64GB of RAM and two NVIDIA 3090 RTX GPUs.

When performing semantic segmentation using convolutional neural networks, GPU memory is often a bottleneck. Due to this limitation there is a trade off between batch size, which is the number of images used in each training update and patch size, which is the size of the images used during training. Larger input patches allow more context to be considered for each voxel or pixel classification decision and have been found to improve accuracy [13]. Therefore we used an input patch size of 64x256x256 for all experiments as this was the largest we could fit in GPU memory. However as such large input patches take up more GPU memory they force a reduction in batch size. Therefore we used a batch size of 2 for all experiments with one instance (input patch) on each GPU, utilising a data-parallel approach, meaning the training batch is split across the GPUs. Small batch sizes can be problematic for the commonly used batch normalisation method [14, 36]. Therefore we used group normalisation [36] after each layer as it performs well when small batch sizes are used and has been found to be effective for 3D medical image segmentation tasks [21].

We use a loss function which is a combination of dice [30] and cross-entropy as this has been found to be effective when dealing with class imbalanced datasets [27, 31]. Although in [9] the authors used cross-entropy with importance weights for their main experiments, they mentioned that they also found a combination of cross-entropy and dice loss to both stabilise and accelerate the training process. Another disadvantage of cross-entropy as opposed to dice loss is that organ specific importance weights require manual tuning. We used zero padding in the convolution operations to allow our 3D network to produce an output segmentation with the same size as the input patch.

For all experiments we used the Adam optimiser [16] with a learning rate of 0.0001. For each training run we initialise the weights using He [11] initialisation. We used check-pointing and early stopping [20] to mitigate over-fitting. Check-pointing involves saving the model weights to disk during the training run. We computed the dice on the validation set at the end of each epoch and only saved models which obtained a new highest dice. There are various way to implement an early stopping procedure [23]. Our stopping criterion used the number of epochs since an improved dice had been found, a parameter which is a commonly referred to as patience. We set patience to 20 for all experiments, thus each training run would stop after 20 epochs had passed since a new highest dice score on the validation set had been obtained.

To mitigate the possibility that the results were due to chance, for each organ and method, training runs were repeated until 10 runs had converged, where convergence was defined as the model having at least 0.1 dice on the validation set after 20 epochs.

The methods compared include a baseline full resolution segmentations approach using 3D patches, a two stage localisation approach and a method in-

volving only organ segmentation, where the ground truth was used to localise (Figure 1). In the following sections we describe the three different approaches we experimented with to evaluate the benefits of localisation.

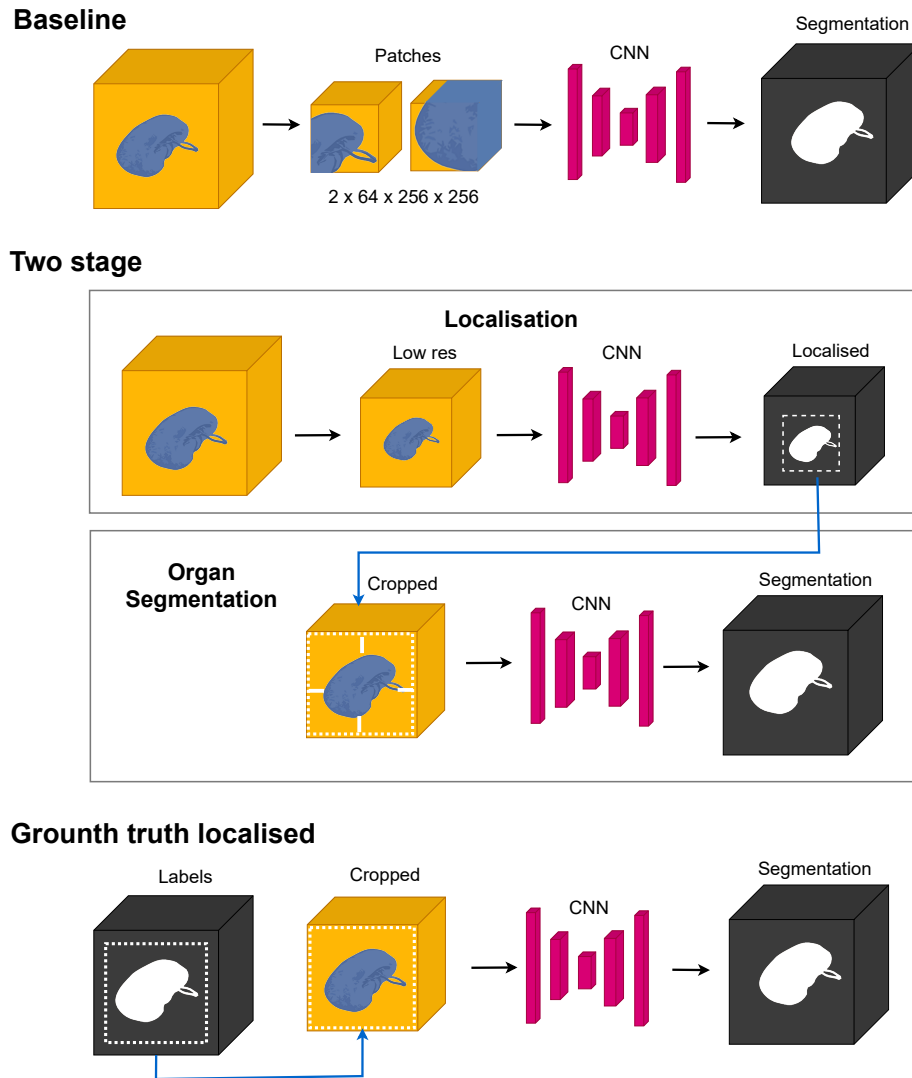


Figure 1: Illustration showing the three different methods compared, including the baseline, two stage involving both a localisation network and organ segmentation network and the organ segmentation network that uses the ground truth to localise.

## Baseline - full resolution segmentation

In order to evaluate the advantages of the two stage localisation process we trained a single stage baseline network. For each training instance we sample a patch with random location within the image and the corresponding location from the annotation. We enforced that at least 80% of the selected patches contained foreground annotation. Such biased instance selection is a relatively common practice as otherwise most patches would not contain foreground which can cause convergence problems.

## Localisation network

In order to train the localisation network we created a low resolution version of the dataset by resizing the images and annotations down to a half their width and height and a third of their depth. We then trained the network to predict the annotations which were also resized to match the reduced resolution images. We created these low res images using the `resize` function from `scikit-image` [33] (Version 0.17.2).

## Organ segmentation network

To train the organ segmentation network, we first created a dataset of images and annotations which were cropped by taking the region of the image including the organ with 15 voxels padding on each side to include some background context. To ensure enough padding was included on each side of the organ, even if the organ was at the edge of an image, the images were zero padded by 15 voxels on each side before cropping to the organ. The organ segmentation network was trained independently using these cropped versions of the original images and ground truth annotations, without regard to the output of any particular localisation network.

## Ground truth localisation

We also evaluated an approach using a localisation stage which utilises the ground truth labels. We do this to access the advantages of localisation given an accurate bounding box.

## Two stage localisation & segmentation pipeline

In order to segment the full resolution image with a preliminary localisation step we implemented a two stage process. We first computed a low res version of the image and then segmented it using the localisation network. We then identified the organ as the largest connected foreground region in the low res segmentation. We then segmented the corresponding region in the full resolution image with padding on each side of the organ as described in the above *Organ segmentation network* section. To perform this two stage segmentation, we pairwise couple

the localisation networks with the organ segmentation networks chronologically, thus the  $i$ 'th organ network trained is coupled with the  $i$ 'th localisation network.

## Metrics

During training we computed dice on both the training and validation data. For the final model that was automatically selected at the end of the training run, dice was computed on both the randomly selected validation and test sets using the full resolution segmentations and annotations.

The two sided t-test as implemented in SciPy [34] (Version 1.5.4) was used for testing for significant differences between the accuracy of the methods on both the validation and test datasets. We also record time for each of the training runs to converge.

## Results

### Training

Table 2: Average training time (minutes) for each of the three types of networks for each of the organs.

	baseline	low res	organ
spleen	74.9	10.8	10.1
pancreas	477.6	65.1	91.2
prostate	6.4	2.0	2.2
liver	253.2	42.8	110.0
heart	22.2	3.7	2.5

For each organ, the baseline approach is substantially slower than the other methods and for all organs takes longer to converge than both the low res and organ networks combined (Table 2).

Both the baseline method and low res networks had less stable performance during training compared to the organ network, with larger fluctuations in the dice (Figure 2). The organ segmentation network always converged (Figure 3a). With the baseline and low res networks, convergence is similarly likely, with 83% of the baseline training runs and 85% of the low res training runs converging. The varying rates of convergence (Figure 3) reflect the difference seen in training stability (Figure 2).

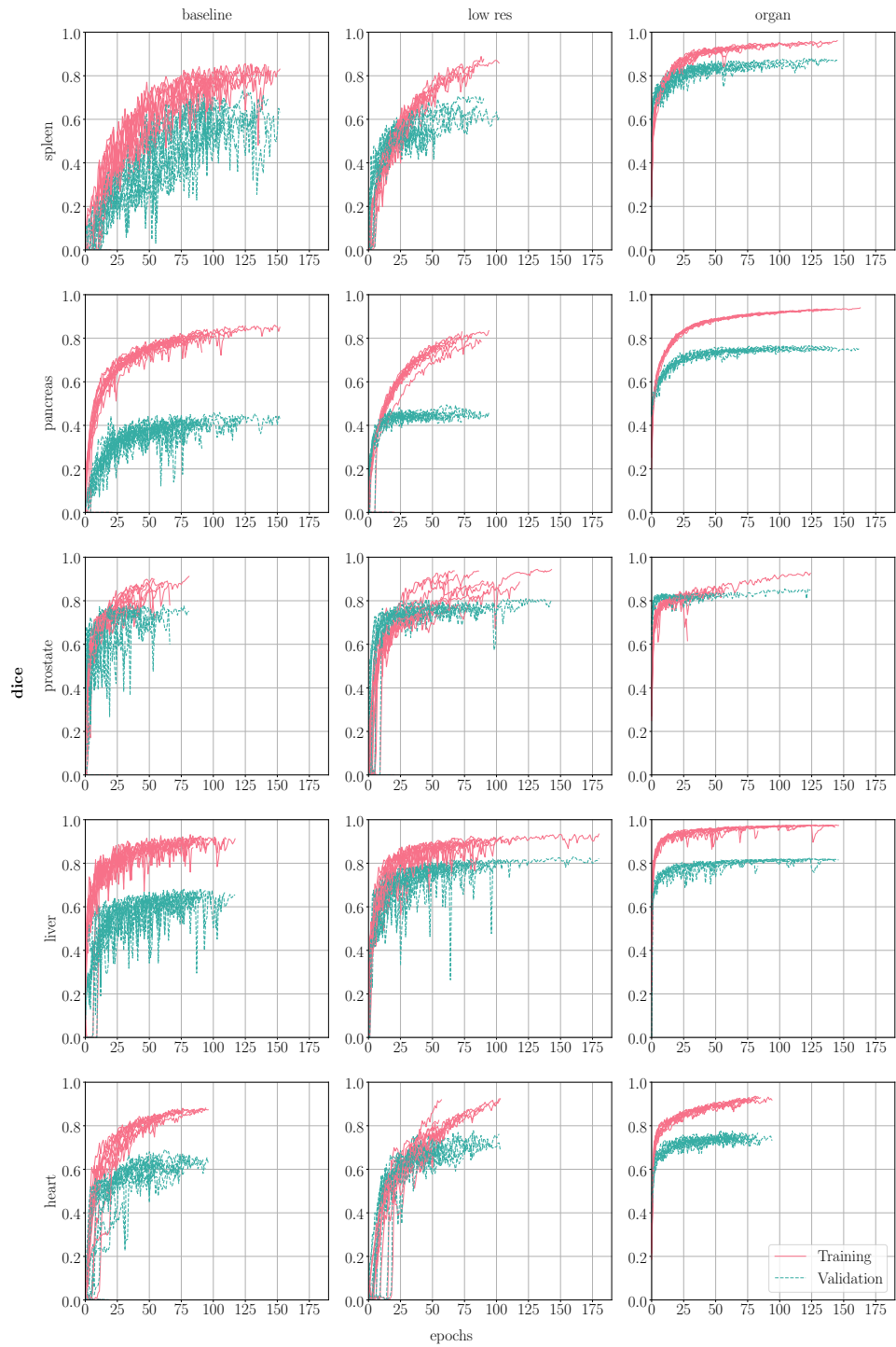


Figure 2: Validation and training dice are shown for each epoch for each of the 10 training runs for each organ and for each method, resulting in 150 training runs in total. Only training runs which successfully converged are shown.

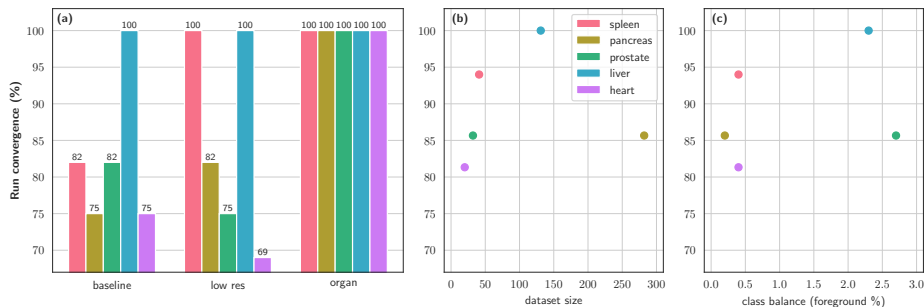


Figure 3: Convergence rate for (a) each method and organ, (b) as a function of dataset size and (c) as a function of class balance (average foreground percent).

## Validation

Table 3: Average dice on the validation set for the baseline network compared to the two stage approach with both predicted and ground truth localisation. Values which are significantly higher than the baseline are shown in bold.

	baseline	two stage	ground truth localised
spleen	0.6491 $\pm$ 0.0997	<b>0.8142 <math>\pm</math> 0.0221</b>	<b>0.8619 <math>\pm</math> 0.0092</b>
pancreas	0.4372 $\pm$ 0.0148	<b>0.6674 <math>\pm</math> 0.0146</b>	<b>0.7564 <math>\pm</math> 0.0096</b>
prostate	0.7744 $\pm$ 0.0109	0.7699 $\pm$ 0.0149	<b>0.8323 <math>\pm</math> 0.0076</b>
liver	0.6661 $\pm$ 0.0188	0.7044 $\pm$ 0.0694	<b>0.7807 <math>\pm</math> 0.1061</b>
heart	0.6547 $\pm$ 0.0239	<b>0.7018 <math>\pm</math> 0.0281</b>	<b>0.7612 <math>\pm</math> 0.0087</b>

For the validation sets, the dice was significantly higher for the two stage approach compared to the baseline method for the heart ( $p < 0.001$ ), spleen ( $p < 0.001$ ) and pancreas ( $p < 0.001$ ). For the liver, although the two stage approach appears it may offer some improvements, the difference was not significant ( $p = 0.11$ ). For the prostate there was no significant difference ( $p = 0.44$ ).

On the validation set, the difference between the ground truth localised method and baseline was significant for the liver ( $p < 0.05$ ) and highly significant for the heart, spleen, pancreas and prostate ( $p < 0.001$ ). For all organs except the liver ( $p = 0.07$ ), the benefits of ground truth localization are significant compared to using the localization network to provide the cropped region ( $p < 0.001$ ).



## Test

Table 4: Average dice on the test set for the baseline network compared to the two stage approach with both predicted and ground truth localisation. Values which are significantly higher than the baseline are shown in bold.

	baseline	two stage	ground truth localised
spleen	0.4433 $\pm$ 0.1162	<b>0.6503 <math>\pm</math> 0.0538</b>	<b>0.8255 <math>\pm</math> 0.0086</b>
pancreas	0.4366 $\pm$ 0.0205	<b>0.6519 <math>\pm</math> 0.0136</b>	<b>0.7397 <math>\pm</math> 0.0063</b>
prostate	0.797 $\pm$ 0.0342	0.7204 $\pm$ 0.0244	<b>0.8361 <math>\pm</math> 0.0145</b>
liver	0.6039 $\pm$ 0.0214	0.6096 $\pm$ 0.0664	<b>0.7156 <math>\pm</math> 0.1028</b>
heart	0.5764 $\pm$ 0.0311	<b>0.623 <math>\pm</math> 0.0523</b>	<b>0.7508 <math>\pm</math> 0.0178</b>

On the test set, the two stage dice score was higher than the baseline for the spleen ( $p < 0.001$ ), pancreas ( $p < 0.001$ ) and heart ( $p < 0.05$ ). For the liver the difference was not significant ( $p = 0.8$ ). The test set dice was significantly higher with the baseline approach compared to the two stage method for the prostate ( $p < 0.001$ ).

When using the ground truth labels to localise, the increase in organ network dice compared to the baseline was highly significant for the heart, spleen and pancreas ( $p < 0.001$ ) and significant for the prostate and liver ( $p < 0.05$ ).

The benefits of ground truth localization were also highly significant compared to using the localization network to provide the cropped region for the heart, spleen, pancreas and prostate ( $p < 0.001$ ) and significant for the liver ( $p < 0.05$ ). We found that smaller organs, as a percentage of scanned region tend to benefit more from localisation (Figure 4).

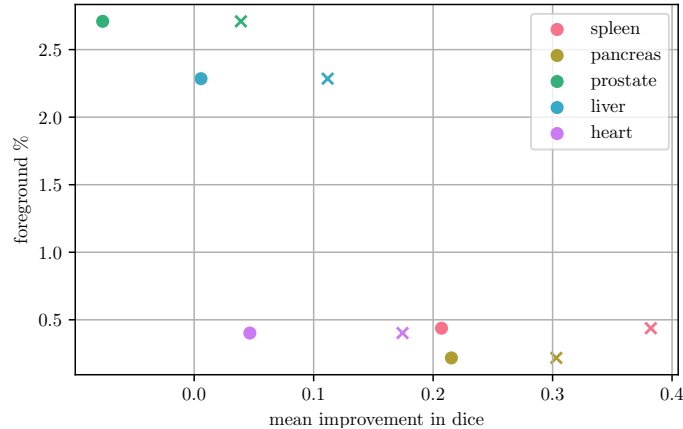


Figure 4: Benefit of localisation for each of the datasets for both predicted localisation region (o) and when the ground truth location is provided (x). The mean improvement in dice is calculated by subtracting the mean baseline dice from the mean localised dice. Foreground % is the percentage of the voxels in a scan that belong to the organ as opposed to the background, where background is considered as all voxels outside of that particular organ.

## Discussion & Conclusion

Although the significant improvements in dice for the majority of datasets confirm our hypothesis that localisation improves organ at risk segmentation accuracy, the baseline performed stronger than expected in comparison to the two stage localisation approach, even out-performing the localisation approach on the prostate test set.

The mean organ volume as a percentage of total image volume ranges from 0.2% for the pancreas to 2.7% for the prostate. This represents an extreme class imbalance, particularly for the pancreas, spleen and left atrium. Class imbalance is known to have detrimental effects on the performance of machine learning models [18] and convolutional neural networks in particular [4]. If not addressed, a class imbalance problem may lead to algorithms tending to predict only the majority class [7]. Gros et al. [10] argue a two stage approach involving localisation is able to mitigate issues caused by class imbalanced data. The trend of an increased benefit of localisation for smaller organs (Figure 4) is expected, because for smaller organs the class balance issue becomes more severe and if the organ becomes large enough there will be negligible difference between the baseline and localisation approaches.

One explanation for the good performance of the baseline could be the random selection of patches during the baseline training procedure. This ran-

dom selection could have provided some augmentation benefits similar to random cropping. When the organ segmentation network encountered unexpected anomalies it may have been less equipped to handle them. Xu et al. [38] trained an organ segmentation network using a region containing the organ of interest but with variation in the amount of padding around it. Varying the amount of context around each organ during training may be key to a two-stage localisation network that provides consistent advantages in accuracy compared to the single stage baseline method.

The baseline and low res network training instability, including fluctuations in dice (Figure 2) is likely related to the challenges with class imbalance. Although the baseline network had biased instance selection to include foreground batches more frequently, its task was likely more complicated compared to cropped organ segmentation as the baseline network must learn to segment regions further away from the organ. For the baseline approach, the patches used in training will have also been less consistent, including varying amounts of the organ of interest or sometimes only background regions.

The heart (left atrium) had the lowest rate of convergence on average, which is likely due to it having both a relatively small dataset (Figure 3b) and a large class imbalance (Figure 3c). Our condition for convergence was based on accuracy, which typically increases with training dataset size [12]. An exception is the pancreas, with the largest dataset, yet a convergence rate of only around 85% (Figure 3b), which may be due to the high class imbalance in this dataset (Figure 3c).

Reduction in model training time is critical for both workflow optimisation and carbon footprint [1]. Slow training may also hinder novel interactive-machine-learning approaches that depend on model adaptation to support a feedback loop between annotator and model [29, 28, 35, 26]. We found that the baseline method had slower convergence and longer training time compared to the localisation approach, even when considering that the localisation approach involved training two networks (Table 2). The slow convergence of patch based training in comparison to other approaches has been observed in previous work evaluating methods for brain tumour segmentation [3].

A potential drawback of the two stage localisation approach is the additional complexity of training two networks. A potential limitation to the network architecture used in this study is the use of zero-padding to ensure that the network input and output had consistent size. In some cases zero-padding has been found to increase errors on the edge of a patch by as much as 35% [13].

The consistent benefits of using ground truth to localise the region for the organ segmentation network (Table 4) motivate the use of a manual bounding box in cases where accuracy improvements are required for smaller organs, an approach that has been used for prior studies in interactive machine learning for organ at risk segmentation [29]. Manual localisation would also be feasible with interactive segmentation methods, such as the approach proposed by Rasmussen et al. [24] where organ extremities are input to guide the predicted contour.

Our results show the advantages of both manual and automatic localisation for organ at risk segmentation in terms of both training time, convergence rate

and segmentation accuracy, especially for smaller organs where class imbalance causes challenges for conventional approaches to segmentation model training.

## References

- [1] Lasse F. Wolff Anthony, Benjamin Kanding, and Raghavendra Selvan. Carbontracker: Tracking and Predicting the Carbon Footprint of Training Deep Learning Models. 2020. doi: 10.48550/ARXIV.2007.03051.
- [2] Michela Antonelli, Annika Reinke, Spyridon Bakas, Keyvan Farahani, AnnetteKopp-Schneider, Bennett A. Landman, Geert Litjens, Bjoern Menze, Olaf Ronneberger, Ronald M. Summers, Bram van Ginneken, Michel Bilello, Patrick Bilic, Patrick F. Christ, Richard K. G. Do, Marc J. Gollub, Stephan H. Heckers, Henkjan Huisman, William R. Jarnagin, Maureen K. McHugo, Sandy Napel, Jennifer S. Goli Pernicka, Kawal Rhode, Catalina Tobon-Gomez, Eugene Vorontsov, Henkjan Huisman, James A. Meakin, Sebastien Ourselin, Manuel Wiesentfarth, Pablo Arbelaez, Byeonguk Bae, Sihong Chen, Laura Daza, Jianjiang Feng, Baochun He, Fabian Isensee, Yuanfeng Ji, Fucang Jia, Namkug Kim, Ildoo Kim, Dorit Merhof, Akshay Pai, Beomhee Park, Mathias Perslev, Ramin Rezaifar, Oliver Rippel, Ignacio Sarasua, Wei Shen, Jaemin Son, Christian Wachinger, Liansheng Wang, Yan Wang, Yingda Xia, Daguang Xu, Zhanwei Xu, Yefeng Zheng, Amber L. Simpson, Lena Maier-Hein, and M. Jorge Cardoso. The Medical Segmentation Decathlon. *Nature Communications*, 13(1):4128, July 2022. ISSN 2041-1723. doi: 10.1038/s41467-022-30695-9.
- [3] David Bouget, André Pedersen, Sayied Abdol Mohieb Hosainey, Ole Solheim, and Ingerid Reinertsen. Meningioma Segmentation in T1-Weighted MRI Leveraging Global Context and Attention Mechanisms. *Frontiers in Radiology*, 1, 2021. ISSN 2673-8740.
- [4] Mateusz Buda, Atsuto Maki, and Maciej A. Mazurowski. A systematic study of the class imbalance problem in convolutional neural networks. *Neural Networks*, 106:249–259, October 2018. ISSN 08936080. doi: 10.1016/j.neunet.2018.07.011.
- [5] Carlos E. Cardenas, Jinzhong Yang, Brian M. Anderson, Laurence E. Court, and Kristy B. Brock. Advances in Auto-Segmentation. *Seminars in Radiation Oncology*, 29(3):185–197, July 2019. ISSN 1053-4296. doi: 10.1016/j.semradonc.2019.02.001.
- [6] Özgün Çiçek, Ahmed Abdulkadir, Soeren S. Lienkamp, Thomas Brox, and Olaf Ronneberger. 3D U-Net: Learning Dense Volumetric Segmentation from Sparse Annotation. *arXiv:1606.06650 [cs]*, June 2016.
- [7] Chris Drummond and Robert C. Holte. Severe Class Imbalance: Why Better Algorithms Aren't the Answer. In João Gama, Rui Camacho,

- Pavel B. Brazdil, Alípio Mário Jorge, and Luís Torgo, editors, *Machine Learning: ECML 2005*, Lecture Notes in Computer Science, pages 539–546, Berlin, Heidelberg, 2005. Springer. ISBN 978-3-540-31692-3. doi: 10.1007/11564096\_52.
- [8] Gary A. Ezzell, James M. Galvin, Daniel Low, Jatinder R. Palta, Isaac Rosen, Michael B. Sharpe, Ping Xia, Ying Xiao, Lei Xing, Cedric X. Yu, IMRT subcommittee, and AAPM Radiation Therapy committee. Guidance document on delivery, treatment planning, and clinical implementation of IMRT: Report of the IMRT Subcommittee of the AAPM Radiation Therapy Committee. *Medical Physics*, 30(8):2089–2115, August 2003. ISSN 0094-2405. doi: 10.1118/1.1591194.
- [9] Xue Feng, Kun Qing, Nicholas J. Tustison, Craig H. Meyer, and Quan Chen. Deep convolutional neural network for segmentation of thoracic organs-at-risk using cropped 3D images. *Medical Physics*, 46(5):2169–2180, 2019. ISSN 2473-4209. doi: 10.1002/mp.13466.
- [10] Charley Gros, Benjamin De Leener, Atef Badji, Josefina Maranzano, Dominique Eden, Sara M. Dupont, Jason Talbott, Ren Zhuoquiong, Yaou Liu, Tobias Granberg, Russell Ouellette, Yasuhiko Tachibana, Masaaki Hori, Kouhei Kamiya, Lydia Chougar, Leszek Stawiarz, Jan Hillert, Elise Bannier, Anne Kerbrat, Gilles Edan, Pierre Labauge, Virginie Callot, Jean Pelletier, Bertrand Audoin, Henitsoa Rasoanandrianina, Jean-Christophe Brisset, Paola Valsasina, Maria A. Rocca, Massimo Filippi, Rohit Bakshi, Shahamat Tauhid, Ferran Prados, Marios Yiannakas, Hugh Kearney, Olga Ciccarelli, Seth Smith, Constantina Andrada Treaba, Caterina Mainero, Jennifer Lefeuvre, Daniel S. Reich, Govind Nair, Vincent Auclair, Donald G. McLaren, Allan R. Martin, Michael G. Fehlings, Shahabeddin Vahdat, Ali Khatibi, Julien Doyon, Timothy Shepherd, Erik Charlson, Sridar Narayanan, and Julien Cohen-Adad. Automatic segmentation of the spinal cord and intramedullary multiple sclerosis lesions with convolutional neural networks. *NeuroImage*, 184:901–915, January 2019. ISSN 1053-8119. doi: 10.1016/j.neuroimage.2018.09.081.
- [11] Kaiming He, Xiangyu Zhang, Shaoqing Ren, and Jian Sun. Delving Deep into Rectifiers: Surpassing Human-Level Performance on ImageNet Classification. *arXiv:1502.01852 [cs]*, February 2015.
- [12] Edward G. A. Henderson, Marcel van Herk, and Eliana M. Vasquez Osorio. The impact of training dataset size and ensemble inference strategies on head and neck auto-segmentation. 2023. doi: 10.48550/ARXIV.2303.17318.
- [13] Bohao Huang, Daniel Reichman, Leslie M. Collins, Kyle Bradbury, and Jordan M. Malof. Tiling and Stitching Segmentation Output for Remote Sensing: Basic Challenges and Recommendations. *arXiv:1805.12219 [cs]*, February 2019.

- [14] Sergey Ioffe and Christian Szegedy. Batch Normalization: Accelerating Deep Network Training by Reducing Internal Covariate Shift. *arXiv:1502.03167 [cs]*, March 2015.
- [15] Leo Joskowicz, D. Cohen, N. Caplan, and J. Sosna. Inter-observer variability of manual contour delineation of structures in CT. *European Radiology*, 29(3):1391–1399, March 2019. ISSN 1432-1084. doi: 10.1007/s00330-018-5695-5.
- [16] Diederik P. Kingma and Jimmy Ba. Adam: A Method for Stochastic Optimization. *arXiv:1412.6980 [cs]*, January 2017.
- [17] Denis Kutnar, Bas H. M. van der Velden, Marta Girones Sanguesa, Mirjam I. Geerlings, J. Matthijs Biesbroek, and Hugo J. Kuijf. MixLacune: Segmentation of lacunes of presumed vascular origin. 2021. doi: 10.48550/ARXIV.2108.02483.
- [18] Charles X. Ling and Victor S. Sheng. Class Imbalance Problem. In Claude Sammut and Geoffrey I. Webb, editors, *Encyclopedia of Machine Learning*, pages 171–171. Springer US, Boston, MA, 2010. ISBN 978-0-387-30164-8. doi: 10.1007/978-0-387-30164-8\_110.
- [19] Thomas Rockwell Mackie, Jeff Kapatoes, Ken Ruchala, Weiguo Lu, Chuan Wu, Gustavo Olivera, Lisa Forrest, Wolfgang Tome, Jim Welsh, Robert Jeraj, Paul Harari, Paul Reckwerdt, Bhudatt Paliwal, Mark Ritter, Harry Keller, Jack Fowler, and Minesh Mehta. Image guidance for precise conformal radiotherapy. *International Journal of Radiation Oncology, Biology, Physics*, 56(1):89–105, May 2003. ISSN 0360-3016. doi: 10.1016/S0360-3016(03)00090-7.
- [20] Nelson Morgan and Hervé Bourlard. Generalization and parameter estimation in feedforward nets: Some experiments. In *Advances in Neural Information Processing Systems*, pages 630–637, 1990.
- [21] Andriy Myronenko. 3D MRI Brain Tumor Segmentation Using Autoencoder Regularization. In Alessandro Crimi, Spyridon Bakas, Hugo Kuijf, Farahani Keyvan, Mauricio Reyes, and Theo van Walsum, editors, *Brainlesion: Glioma, Multiple Sclerosis, Stroke and Traumatic Brain Injuries*, Lecture Notes in Computer Science, pages 311–320, Cham, 2019. Springer International Publishing. ISBN 978-3-030-11726-9. doi: 10.1007/978-3-030-11726-9\_28.
- [22] Adam Paszke, Sam Gross, Soumith Chintala, Gregory Chanan, Edward Yang, Zachary DeVito, Zeming Lin, Alban Desmaison, Luca Antiga, and Adam Lerer. Automatic differentiation in PyTorch. page 4.
- [23] Lutz Prechelt. Early Stopping — but when? page 15.

- [24] Mathis Ersted Rasmussen, Jasper Albertus Nijkamp, Jesper Grau Eriksen, and Stine Sofia Korreman. A simple single-cycle interactive strategy to improve deep learning-based segmentation of organs-at-risk in head-and-neck cancer. *Physics and Imaging in Radiation Oncology*, 26:100426, April 2023. ISSN 24056316. doi: 10.1016/j.phro.2023.100426.
- [25] Amber L. Simpson, Michela Antonelli, Spyridon Bakas, Michel Bilello, Keyvan Farahani, Bram van Ginneken, Annette Kopp-Schneider, Bennett A. Landman, Geert Litjens, Bjoern Menze, Olaf Ronneberger, Ronald M. Summers, Patrick Bilic, Patrick F. Christ, Richard K. G. Do, Marc Golub, Jennifer Golia-Pernicka, Stephan H. Heckers, William R. Jarnagin, Maureen K. McHugo, Sandy Napel, Eugene Vorontsov, Lena Maier-Hein, and M. Jorge Cardoso. A large annotated medical image dataset for the development and evaluation of segmentation algorithms, February 2019.
- [26] A. Smith, J. Petersen, I. Wahlstedt, S.L. Risumlund, M.V.O. Felter, V.N. Hansen, and I.R. Vogelius. PD-0065 Corrective-annotation auto-completion enables faster organ contouring. *Radiotherapy and Oncology*, 170:S38–S39, May 2022. ISSN 01678140. doi: 10.1016/S0167-8140(22)02735-9.
- [27] Abraham George Smith, Jens Petersen, Raghavendra Selvan, and Camilla Ruø Rasmussen. Segmentation of roots in soil with U-Net. *Plant Methods*, 16(1):13, February 2020. ISSN 1746-4811. doi: 10.1186/s13007-020-0563-0.
- [28] Abraham George Smith, Eusun Han, Jens Petersen, Niels Alvin Faircloth Olsen, Christian Giese, Miriam Athmann, Dorte Bodin Dresbøll, and Kristian Thorup-Kristensen. RootPainter: Deep learning segmentation of biological images with corrective annotation. *New Phytologist*, 236(2):774–791, 2022. ISSN 1469-8137. doi: 10.1111/nph.18387.
- [29] Abraham George Smith, Jens Petersen, Cynthia Terrones-Campos, Anne Kiil Berthelsen, Nora Jarrett Forbes, Sune Darkner, Lena Specht, and Ivan Richter Vogelius. RootPainter3D: Interactive-machine-learning enables rapid and accurate contouring for radiotherapy. *Medical Physics*, 49(1):461–473, 2022. ISSN 2473-4209. doi: 10.1002/mp.15353.
- [30] Carole H. Sudre, Wenqi Li, Tom Vercauteren, Sébastien Ourselin, and M. Jorge Cardoso. Generalised Dice overlap as a deep learning loss function for highly unbalanced segmentations. *arXiv:1707.03237 [cs]*, 10553: 240–248, 2017. doi: 10.1007/978-3-319-67558-9\_28.
- [31] Saeid Asgari Taghanaki, Yefeng Zheng, S. Kevin Zhou, Bogdan Georgescu, Puneet Sharma, Daguang Xu, Dorin Comaniciu, and Ghassan Hamarneh. Combo Loss: Handling Input and Output Imbalance in Multi-Organ Segmentation. *arXiv:1805.02798 [cs]*, October 2018.
- [32] Hao Tang, Xuming Chen, Yang Liu, Zhipeng Lu, Junhua You, Mingzhou Yang, Shengyu Yao, Guoqi Zhao, Yi Xu, Tingfeng Chen, Yong Liu, and

- Xiaohui Xie. Clinically applicable deep learning framework for organs at risk delineation in CT images. *Nature Machine Intelligence*, 1(10):480–491, October 2019. ISSN 2522-5839. doi: 10.1038/s42256-019-0099-z.
- [33] Stéfan van der Walt, Johannes L. Schönberger, Juan Nunez-Iglesias, François Boulogne, Joshua D. Warner, Neil Yager, Emmanuelle Gouillart, and Tony Yu. Scikit-image: Image processing in Python. *PeerJ*, 2:e453, June 2014. ISSN 2167-8359. doi: 10.7717/peerj.453.
- [34] Pauli Virtanen, Ralf Gommers, Travis E. Oliphant, Matt Haberland, Tyler Reddy, David Cournapeau, Evgeni Burovski, Pearu Peterson, Warren Weckesser, Jonathan Bright, Stéfan J. van der Walt, Matthew Brett, Joshua Wilson, K. Jarrod Millman, Nikolay Mayorov, Andrew R. J. Nelson, Eric Jones, Robert Kern, Eric Larson, C. J. Carey, İlhan Polat, Yu Feng, Eric W. Moore, Jake VanderPlas, Denis Laxalde, Josef Perktold, Robert Cimrman, Ian Henriksen, E. A. Quintero, Charles R. Harris, Anne M. Archibald, Antônio H. Ribeiro, Fabian Pedregosa, and Paul van Mulbregt. SciPy 1.0: Fundamental algorithms for scientific computing in Python. *Nature Methods*, 17(3):261–272, March 2020. ISSN 1548-7105. doi: 10.1038/s41592-019-0686-2.
- [35] Zixiang Wei, Jintao Ren, Stine Sofia Korreman, and Jasper Nijkamp. Towards interactive deep-learning for tumour segmentation in head and neck cancer radiotherapy. *Physics and Imaging in Radiation Oncology*, 25: 100408, January 2023. ISSN 2405-6316. doi: 10.1016/j.phro.2022.12.005.
- [36] Yuxin Wu and Kaiming He. Group Normalization. In *Proceedings of the European Conference on Computer Vision (ECCV)*, pages 3–19, 2018.
- [37] X. Xu, F. Zhou, B. Liu, and X. Bai. Multiple Organ Localization in CT Image Using Triple-Branch Fully Convolutional Networks. *IEEE Access*, 7: 98083–98093, 2019. ISSN 2169-3536. doi: 10.1109/ACCESS.2019.2930417.
- [38] Xuanang Xu, Fugen Zhou, Bo Liu, Dongshan Fu, and Xiangzhi Bai. Efficient Multiple Organ Localization in CT Image using 3D Region Proposal Network. *IEEE transactions on medical imaging*, January 2019. ISSN 1558-254X. doi: 10.1109/TMI.2019.2894854.
- [39] Jinzhong Yang, Harini Veeraraghavan, Samuel G. Armato, Keyvan Farahani, Justin S. Kirby, Jayashree Kalpathy-Kramer, Wouter van Elmpt, Andre Dekker, Xiao Han, Xue Feng, Paul Aljabar, Bruno Oliveira, Brent van der Heyden, Leonid Zamdborg, Dao Lam, Mark Gooding, and Gregory C. Sharp. Autosegmentation for thoracic radiation treatment planning: A grand challenge at AAPM 2017. *Medical Physics*, 45(10):4568–4581, October 2018. ISSN 2473-4209. doi: 10.1002/mp.13141.